

Constrained Group Relative Policy Optimization

Roger Girgis ^{*1 2} Rodrigue de Schaezen ^{*1 3} Luke Rowe ^{1 3} Azalée Robitaille ^{1 3} Christopher Pal ^{1 2 3 4}
 Liam Paull ^{1 3 4}

Abstract

While Group Relative Policy Optimization (GRPO) has emerged as a scalable framework for critic-free policy learning, extending it to settings with explicit behavioral constraints remains underexplored. We introduce Constrained GRPO, a Lagrangian-based extension of GRPO for constrained policy optimization. Constraints are specified via indicator cost functions, enabling direct optimization of violation rates through a Lagrangian relaxation. We show that a naive multi-component treatment in advantage estimation can break constrained learning: mismatched component-wise standard deviations distort the relative importance of the different objective terms, which in turn corrupts the Lagrangian signal and prevents meaningful constraint enforcement. We formally derive this effect to motivate our scalarized advantage construction that preserves the intended trade-off between reward and constraint terms. Experiments in a toy gridworld confirm the predicted optimization pathology and demonstrate that scalarizing advantages restores stable constraint control. In addition, we evaluate Constrained GRPO on robotics tasks, where it improves constraint satisfaction while increasing task success, establishing a simple and effective recipe for constrained policy optimization in embodied AI domains that increasingly rely on large multimodal foundation models.

1. Introduction

Recent progress in reinforcement learning (RL) has shown that large multimodal models can be optimized with outcome-based signals. This has enabled the finetuning of models on mathematical reasoning tasks (Cobbe et al., 2021; Wei et al., 2022; Lewkowycz et al., 2022), embod-

ied decision making (Zhang et al., 2025b), among other domains where success can be evaluated with programmatic or learned rewards. Group Relative Policy Optimization (GRPO) (Shao et al., 2024) removes the reliance on a critic for advantage estimation by a within-group normalization of the rewards obtained over multiple sampled outputs for the same query. The critic-free structure of GRPO is appealing when training or deploying a value function is difficult.

Existing GRPO-based methods have largely approached multi-objective optimization through manually weighting the importance of different reward terms (Li et al., 2025b; Ichihara et al., 2025; Liu et al., 2026). In contrast, the constrained policy optimization literature offers a principled framework, namely Constrained Markov Decision Processes (CMDPs), for enforcing behavioural preferences and constraints by explicitly defining thresholds on behaviours rather than employing fixed weights. However, GRPO has not yet been integrated into a constrained optimization framework to yield reliable constraint enforcement. In this work, we propose *Constrained GRPO*, a constrained policy optimization framework employing GRPO as the policy optimization algorithm. Within our framework, we specify desirable behaviours with indicator cost functions (Roy et al., 2021) and enforce target behaviour rates (in percentage) using a Lagrangian relaxation with learned multipliers.

A central challenge arises from the interaction between Lagrangian methods and GRPO’s advantage estimation through within-group standardization. A simple approach is to first *scalarize rewards*, i.e., combine reward and cost terms into a single scalar value using the current multipliers, and then apply the within-group standardization. However, we show that this seemingly innocuous choice can deteriorate the constrained optimization: the group standardization induces an implicit, covariance-dependent reweighting of the terms, distorting the intended relative importance prescribed by the Lagrange multipliers. We provide a mathematical analysis of this phenomenon and illustrate the resulting distortion in Figure 1. Motivated by this analysis, Constrained GRPO employs *scalarizing advantages*, i.e., standardize each component within group first, and then combine the standardized components using the Lagrangian multipliers. By construction, this design preserves the intended prescription of the multipliers by preventing the

^{*}Equal contribution ¹Mila - Quebec AI Institute ²École Polytechnique de Montréal ³Université de Montréal ⁴CIFAR AI Chair. Correspondence to: Roger Girgis <girgisro@mila.quebec>.

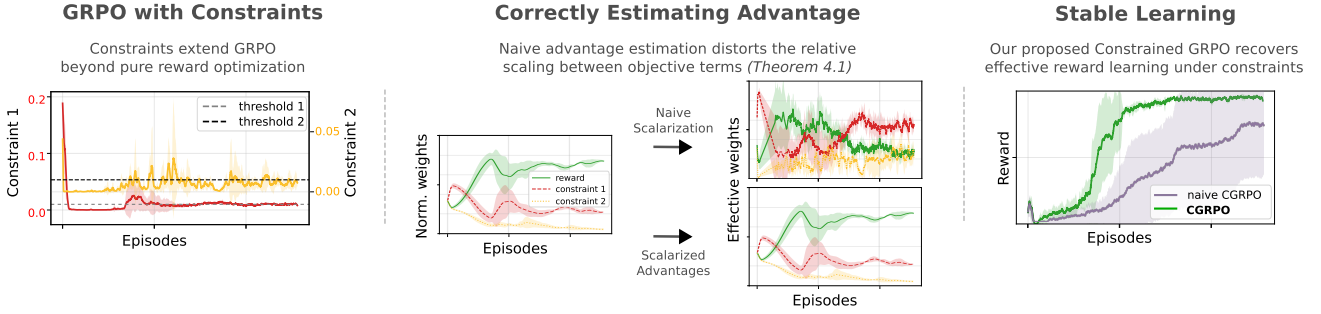


Figure 1. Overview of our proposed approach. We extend GRPO to constrained policy optimization by enforcing user-specified behavioral constraints with thresholds (left). Naively scalarizing reward distorts reward–constraint trade-offs, producing inconsistent effective weights (middle; e.g., red/green swap). Scalarized advantages preserves multiplier semantics, yielding stable learning and effective constraint enforcement (right).

within-group scales and correlations from implicitly reshaping the trade-off, a property we illustrate in our experiments. Prior and concurrent work has also found advantage scalarization beneficial in the realm of multi-objective GRPO (Li et al., 2025b; Ichihara et al., 2025); our contribution places this observation in the context of constrained optimization, showing why it is essential for effective Lagrangian constraint enforcement under GRPO.

Our main contributions are: (1) We introduce Constrained GRPO, a constrained policy optimization framework built on GRPO, using indicator cost functions, Lagrangian relaxation and scalarizing advantages to effectively enforce behaviour rates without manually tuning reward weights. (2) We analyze the common approach of scalarizing rewards before normalizing, and mathematically show in Theorem 4.1 that it implicitly reweights the components as a function of within-group variances and correlations between terms, distorting the prescribed relative importance encoded by the Lagrangian multipliers. (3) We study the alternative approach of scalarizing advantages and empirically demonstrate improved stability and faithfulness of the behaviour specification in a gridworld environment and a realistic simulation-based autonomous driving setting.

2. Related Work

2.1. Reward Specification

A central motivation for our work is the difficulty of specifying complex behaviours through a single reward function. This challenge has inspired several alternative approaches in the literature. Imitation Learning (Zheng et al., 2021) bypasses reward engineering entirely by using expert demonstrations to define the task. Other methods introduce human feedback during training, either to guide the agent toward desired behaviours (Christiano et al., 2017) or to prevent catastrophic errors during exploration (Saunders et al., 2017). Our approach shares a similar motivation—capturing designer intent more directly—but does so by specifying constraints via indicator functions and thresh-

olds, avoiding the need for demonstrations or continuous human intervention. Another promising direction is the use of natural language to specify tasks (Goyal et al., 2019; MacGlashan et al., 2015). While this can provide a more intuitive interface for human designers, language is inherently ambiguous and can be exploited by agents (reward hacking). Moreover, these methods typically require training an additional language-to-reward model, adding further complexity. Another interesting approach is Inverse Reward Design (Hadfield-Menell et al., 2017; Minderhout et al., 2018; Ratner et al., 2018), which treats the provided reward function as a single observation of the designer’s latent intent and learns a probabilistic model over possible true reward functions. This is particularly useful in settings with changing environments, but our work focuses on fixed-distribution environments where explicit behaviour specification is more appropriate.

2.2. Multi-Objective Optimization with Large Models

In the context of large multimodal (vision-)language models, there is extensive work on safety and multi-objective optimization via reinforcement learning (Moskovitz et al., 2023; Zhang et al., 2025a; Dai et al., 2023; Ji et al., 2025; Bai et al., 2022). For example, Constitutional AI (Bai et al., 2022) can be viewed as balancing multiple objectives—most notably helpfulness and harmlessness—yet in practice these objectives are typically reduced to a single scalar reward and optimized with standard RLHF (Ouyang et al., 2022) pipelines, for instance PPO-style updates (Schulman et al., 2017). Moskovitz et al. (2023) frame composite reward models in RLHF as a constrained optimization problem, enforcing thresholds on individual reward components via a CMDP formulation and using dynamic weight adjustment (i.e., Lagrange multipliers) to mitigate over-optimization. Similarly, Dai et al. (2023) formulate alignment as maximizing reward subject to cost constraints in RLHF, explicitly trading off helpfulness against safety-related costs. Finally, Wang et al. (2024) study multi-objective reward models in RLHF, emphasizing interpretability as a means to help

designers verify adherence to human preferences.

While several recent methods target safety alignment for RL-finetuned (vision-)language models, they are largely developed outside the GRPO setting. More recent work (Li et al., 2025b) train a multi-head reward model that predicts $K=4$ attributes (politeness, meaningfulness, actionability, safety) and then form a single scalar reward via a fixed weighted sum (using $w_k=1$ for all components), before optimizing the resulting objective with GRPO. Ichihara et al. (2025) propose Multi-Objective GRPO (MO-GRPO) to reduce reward-hacking behavior under multiple objectives, and advocate scalarized advantages to equalize the influence of components with different variances. Concurrent to our work, GDPO (Liu et al., 2026) also supports advantage scalarization and emphasizes the difficulty of selecting reward weights that reflect desired priorities, proposing conditional objectives that activate certain terms only once prerequisite scores exceed a minimum threshold. In contrast, we study advantage scalarization through the lens of *constrained* policy optimization. Our goal is to ensure that increases in the Lagrangian multipliers in Constrained GRPO translate into stronger enforcement of the specified behaviors. As shown experimentally, scalarizing advantages provides this property, whereas scalarizing rewards can implicitly reweight objectives and undermine effective Lagrangian optimization.

3. Background

Markov Decision Processes (MDPs). A Markov decision process (MDP) is defined by $(\mathcal{S}, \mathcal{A}, P, R)$ (Sutton & Barto, 2018), where \mathcal{S} is the state space, \mathcal{A} the action space, $P(\cdot | s, a)$ the transition kernel, and $R(s, a)$ the reward function. At time t , the agent samples an action $a_t \sim \pi(\cdot | s_t)$, transitions according to $s_{t+1} \sim P(\cdot | s_t, a_t)$, and receives reward $R(s_t, a_t)$. The trajectory distribution under π and the expected discounted return are

$$p_\pi(\tau) = P_0(s_0) \prod_{t=0}^{T-1} P(s_{t+1} | s_t, a_t) \pi(a_t | s_t),$$

$$J_R(\pi) = \mathbb{E}_{\tau \sim p_\pi} \left[\sum_{t=0}^{T-1} \gamma^t R(s_t, a_t) \right],$$

where the objective is to learn a policy π^* that maximizes the expected discounted return, i.e. $\pi^* = \arg \max_\pi J_R(\pi)$.

Constrained Markov Decision Processes (CMDPs). A constrained MDP (CMDP) augments the MDP objective with K expected cost constraints (Altman, 1999). Given cost functions $C_k : \mathcal{S} \times \mathcal{A} \rightarrow \mathbb{R}$ and thresholds d_k , define

the feasible set of policies as

$$\Pi_C = \left\{ \pi \in \Pi : J_{C_k}(\pi) \leq d_k, \ k = 1, \dots, K \right\},$$

$$J_{C_k}(\pi) = \mathbb{E}_{\tau \sim p_\pi} \left[\sum_{t=0}^{T-1} \gamma^t C_k(s_t, a_t) \right].$$

The constrained optimal policy maximizes return subject to feasibility:

$$\pi^* = \arg \max_{\pi \in \Pi} J_R(\pi) \quad \text{s.t.} \quad J_{C_k}(\pi) \leq d_k, \ k = 1, \dots, K,$$

where stationary *stochastic* policies may be required for optimality (Altman, 1999).

Lagrangian methods. CMDPs are commonly addressed with Lagrangian methods (Achiam et al., 2017; Ray et al., 2019; Stooke et al., 2020; Zhang et al., 2020; 2025b), which cast the problem as a saddle-point optimization (Uzawa et al., 1958; Polyak, 1970; Korpelevich, 1976). These methods introduce nonnegative multipliers $\lambda = \{\lambda_k\}_{k=1}^K \geq 0$, where each λ_k controls the penalty for constraint k and relative emphasis across constraints is determined by ratios such as λ_i/λ_j . The resulting min–max problem is

$$\max_{\pi} \min_{\lambda \geq 0} \mathcal{L}(\pi, \lambda), \quad (1)$$

$$\text{where } \mathcal{L}(\pi, \lambda) = J_R(\pi) - \sum_{k=1}^K \lambda_k (J_{C_k}(\pi) - d_k).$$

A standard approach applies gradient ascent in π and gradient descent in λ (Lin et al., 2020), analogous to training procedures used in GANs (Goodfellow et al., 2014). In practice, such schemes often attain good feasible solutions on CMDP benchmarks (Achiam et al., 2017; Ray et al., 2019; Stooke et al., 2020; Zhang et al., 2020).

Prior work (Roy et al., 2021) employed multiplier normalization:

$$\lambda_k = \frac{\exp(z_k)}{\exp(a_R) + \sum_{k'=1}^K \exp(z_{k'})}, \quad k = 1, \dots, K.$$

which includes a dummy variable a_R for the main reward function such that $\lambda_R := 1 - \sum_{k=1}^K \lambda_k$ and z_k are the unnormalized multipliers. This mechanism ensures that one constraint can dominate the policy updates if necessary while maintaining stability. The policy update now corresponds to optimizing the linearly-combined reward signal,

$$R_c(s, a) = \lambda_R R(s, a) - \sum_{k=1}^K \lambda_k C_k(s, a), \quad (2)$$

and can be carried out with any policy optimization method (e.g., PPO (Schulman et al., 2017), SAC (Haarnoja et al., 2018)). The multiplier update follows

$$\nabla_{\lambda_k} \mathcal{L}(\pi, \lambda) = -(J_{C_k}(\pi) - d_k), \quad (3)$$

typically implemented with a learning rate and a projection onto $\lambda_k \geq 0$ using max-clipping. If constraint k is violated ($J_{C_k} > d_k$), λ_k increases, strengthening its penalty; if it is satisfied ($J_{C_k} < d_k$), λ_k decreases, allowing optimization to focus on return and other active constraints.

Group-Relative Policy Optimization (GRPO). Reinforcement learning has proven effective for finetuning large models, complementing supervised finetuning (SFT): while SFT supports instruction and format adherence, RL finetuning often improves generalization, particularly in out-of-distribution regimes (Chu et al., 2025). Early work used PPO with learned reward models for preference optimization (Ouyang et al., 2022). Assuming access to a queryable scalar reward (e.g., BLEU/ROUGE, verifier-based math checking), Shao et al. (2024) proposed eliminating the value model by estimating advantages within a group of samples. Given a start state s_0 , GRPO samples G candidate trajectories $\{\tau_i\}_{i=1}^G \sim \pi_{\theta_{\text{old}}}$ and standardizes returns with a group-relative baseline:

$$A_i = \frac{R(\tau_i) - \text{mean}(\mathbf{R})}{\text{std}(\mathbf{R})}, \quad \mathbf{R} = [R(\tau_1), \dots, R(\tau_G)].$$

Using A_i , the PPO objective is modified into GRPO:

$$\begin{aligned} \mathcal{J}_{\text{GRPO}}(\theta) &= \mathbb{E}_{\{\tau_i\}_{i=1}^G \sim \pi_{\theta_{\text{old}}}} \left[\frac{1}{G} \sum_{i=1}^G \sum_{t=0}^{T-1} \left\{ \min[b_1 \cdot A_i, b_2 \cdot A_i] - \beta \mathbb{D}_{\text{KL}}[\pi_{\theta} \parallel \pi_{\text{ref}}] \right\} \right], \\ b_1 &= \frac{\pi_{\theta}(a_t^i \mid s_t^i)}{\pi_{\theta_{\text{old}}}(a_t^i \mid s_t^i)}, b_2 = \text{clip} \left(\frac{\pi_{\theta}(a_t^i \mid s_t^i)}{\pi_{\theta_{\text{old}}}(a_t^i \mid s_t^i)}, 1 + \epsilon, 1 - \epsilon \right), \end{aligned}$$

where the KL term directly regularizes the trained policy toward a fixed reference policy π_{ref} , rather than being folded into the reward. GRPO has shown strong performance in mathematical reasoning (Shao et al., 2024) and has also been adopted in various robotics work (Li et al., 2025c; Chen et al., 2025; Pei et al., 2025; Wang et al., 2025).

4. Constrained GRPO

We study multi-objective constrained optimization with GRPO as the underlying policy-gradient algorithm. We consider $K + 1$ objectives: one primary reward and K behavioral constraints, combined via the weighted form in Eq. (2). In large multimodal models, a common practice is to set the weights $\{\lambda_k\}$ manually and keep them fixed throughout training; for example, Ichihara et al. (2025) and Li et al. (2025b) use $\lambda_k = 1$ for all k . In contrast, we formulate the problem in the constrained MDP framework and optimize the behavioral constraints using Lagrangian methods. Our focus is on how to integrate these Lagrangian updates with GRPO’s group-based advantage estimation effectively.

4.1. Proposed Framework

We model each desired behavior k as a constraint and enforce it through a cost function C_k with a target threshold. A key design choice is how to express these thresholds in an intuitive and behavior-agnostic way. Following prior work on direct behavior specification (Roy et al., 2021), we restrict our attention to indicator cost functions, $C_k(s, a) = \mathbb{I}[\text{constraint } k \text{ violated in } (s, a)]$, for which the threshold \tilde{d}_k directly corresponds to a desired behavior rate. For example, requiring an agent to touch lava at most 1% of the time corresponds to setting the behaviour threshold $\tilde{d}_{\text{lava}} = 0.01$.

Beyond choosing the constraint functions, multi-objective optimization requires setting the relative trade-offs between objectives. However, when the feasible policy set is small, achieving constraint satisfaction can require a fine-grained search over $\{\lambda_k\}$, with a full training run per setting (Roy et al., 2021), which is impractical at scale. We therefore adopt the constrained MDP formulation and use Lagrangian methods to adapt the multipliers during training.

We estimate constraint violations from a batch of experience by the empirical average of the cost $C_k(s_i, a_i)$, which weighs all visited state-action pairs equally, independent of their time index in the trajectory. In our experiments, some constraints are measured at the episode level: a violation is recorded if the corresponding event occurs at any time during the episode. We treat per-timestep and per-episode constraints in the same fashion. The Lagrangian parameters are optimized using the update rule in Eq. (3), with $d_k \rightarrow \tilde{d}_k$ and $J_{C_k}(\pi)$ computed as the average over $\{C_k(s_i, a_i)\}_{i=1}^N$.

Advantage estimation. With the updated Lagrange multipliers, a straightforward baseline is to compute a scalar trajectory return by linearly combining reward and costs as in Eq. (2). GRPO advantages are then obtained by standardizing these scalar returns within each group; we call this approach *Scalarized Rewards*. Prior (Ichihara et al., 2025) and concurrent (Liu et al., 2026) work report that this strategy can be suboptimal in multi-objective settings. In the next section, we offer a complementary mathematical analysis demonstrating why, in our framework, it can also undermine effective Lagrangian constraint enforcement.

4.2. Effective Constraint Enforcement with GRPO

Recall that GRPO (Shao et al., 2024) estimates advantages by *within-group standardization*, i.e., subtracting the group mean and dividing by the group standard deviation (Section 3). In the presence of multiple objectives—one main reward and additional behavioral constraints—there are two natural ways to incorporate constraints into GRPO’s advantage computation, each with distinct implications for constraint enforcement.

Scalarized Rewards. In the *Scalarized Rewards* approach, we first form a single scalar signal by linearly combining the main reward and all constraint costs, and then apply GRPO’s within-group standardization to this combined signal (as commonly done in prior work (Li et al., 2025b)). The following result characterizes the resulting advantage in terms of per-component standardized variables.

Theorem 4.1 (Implicit reweighting under scalarized rewards). *Let*

$$\mathbf{x} := \begin{bmatrix} R \\ C_1 \\ \vdots \\ C_K \end{bmatrix} \in \mathbb{R}^{K+1}, \quad \boldsymbol{\lambda} := \begin{bmatrix} \lambda_R \\ \lambda_1 \\ \vdots \\ \lambda_K \end{bmatrix} \in \mathbb{R}^{K+1},$$

and define the scalarized reward $R_S := \boldsymbol{\lambda}^\top \mathbf{x}$. Denote the within-group mean and covariance of \mathbf{x} by $\boldsymbol{\mu} := \mathbb{E}[\mathbf{x}]$ and $\boldsymbol{\Sigma} := \text{Cov}(\mathbf{x})$, respectively, and let

$$\sigma_{R_S} := \sqrt{\text{Var}(R_S)} = \sqrt{\boldsymbol{\lambda}^\top \boldsymbol{\Sigma} \boldsymbol{\lambda}}.$$

Further, define per-component standardizations

$$\mathbf{Z} := \mathbf{D}^{-1}(\mathbf{x} - \boldsymbol{\mu}), \quad \mathbf{D} := \text{diag}(\sigma_R, \sigma_{C_1}, \dots, \sigma_{C_K})$$

$$\sigma_R > 0, \quad \sigma_{C_k} > 0 \quad \forall k \in \{1, \dots, K\},$$

so that

$$Z_R := \frac{R - \mu_R}{\sigma_R},$$

$$Z_{C_k} := \frac{C_k - \mu_{C_k}}{\sigma_{C_k}}, \quad k = 1, \dots, K, \quad (4)$$

where $\mu_{(\cdot)}$ and $\sigma_{(\cdot)}$ denote the within-group mean and standard deviation of the corresponding component. Then the GRPO advantage obtained by standardizing the scalarized reward,

$$A_{\text{ScRew}} := \frac{R_S - \mathbb{E}[R_S]}{\sigma_{R_S}},$$

admits the expansion

$$A_{\text{ScRew}} = \frac{(\mathbf{D}\boldsymbol{\lambda})^\top \mathbf{Z}}{\sigma_{R_S}} = \sum_{j=0}^K \left(\frac{\lambda_j \sigma_j}{\sigma_{R_S}} \right) Z_j, \quad (5)$$

where we index $j = 0$ as the main reward component ($\lambda_0 \equiv \lambda_R$, $\sigma_0 \equiv \sigma_R$) and $j = k$ corresponds to cost C_k . Consequently, the effective contribution of each standardized component Z_j is scaled by $\lambda_j \sigma_j / \sigma_{R_S}$, and therefore depends on within-group scales and (through σ_{R_S}) the full covariance structure $\boldsymbol{\Sigma}$.

The proof is provided in Appendix A. To summarize, our **main observation** is revealed in Eq. (5): under scalarized

rewards, the effective contribution of each standardized component Z_j and the intended trade-offs encoded by the Lagrangian multipliers, $\boldsymbol{\lambda}$, are implicitly distorted by component variances and correlations.

Scalarized Advantage. In our constrained GRPO approach, we first compute a GRPO-style standardized advantage *per component* (reward and each constraint) using the respective component’s within-group mean and standard deviation as done in Eq. (4).

We then form a single advantage by linearly combining these standardized components using their current Lagrangian weights

$$A_{\text{ScAdv}} = \lambda_R Z_R - \sum_{k=1}^K \lambda_k Z_{C_k}, \quad (6)$$

where $\lambda_k, \lambda_R \geq 0$ are Lagrange multipliers associated with constraint k and the reward term, respectively. This yields an advantage signal whose relative trade-offs are explicitly controlled by the multipliers.

5. Illustrative Environment

We begin with an illustrative example in a simple gridworld. An agent is randomly initialized in a 10×10 grid and must navigate to a randomly sampled goal location, receiving a sparse scalar reward upon reaching it. Each episode contains 20% lava tiles; stepping onto lava incurs a penalty (i.e., a cost). In addition, the agent has a battery that depletes at every timestep and incurs a penalty whenever its battery level falls below 10%. The action space consists of five discrete actions: moving in the four cardinal directions or staying in place to recharge. More details are available in Appendix C. Although intentionally minimal, this environment provides a controlled testbed for isolating the differences between *scalarized rewards* and *scalarized advantages* in unconstrained and constrained GRPO.

We first compare these approaches under fixed reward and penalty weights. For simplicity, we restrict the battery-penalty weight to $\lambda_{\text{battery}}^{\text{fixed}} \in \{0.0, 0.1\}$ and sweep the lava-penalty weight over $\lambda_{\text{lava}}^{\text{fixed}} \in \{0.0, 0.01, 0.05, 0.1, 0.2, 0.3, 0.5, 0.7, 1.0\}$. Figure 2 illustrates how performance varies as we sweep $\lambda_{\text{lava}}^{\text{fixed}}$ for the two fixed settings of $\lambda_{\text{battery}}^{\text{fixed}}$. Overall, we observe consistently higher goal-reaching rates with *scalarized advantages*, along with more stable performance across seeds (through smaller error bars). Moreover, *scalarized rewards* tends to unilaterally optimize the lava rate: even the smallest non-zero lava weight, $\lambda_{\text{lava}}^{\text{fixed}} = 0.01$, leads to near-minimal lava visitation. In contrast, *scalarized advantages* provides smoother, more gradual control over the lava rate, which we argue better reflects the intended meaning of the weights. When multiple penalty terms are active ($\lambda_{\text{battery}}^{\text{fixed}} = 0.1$, i.e.,

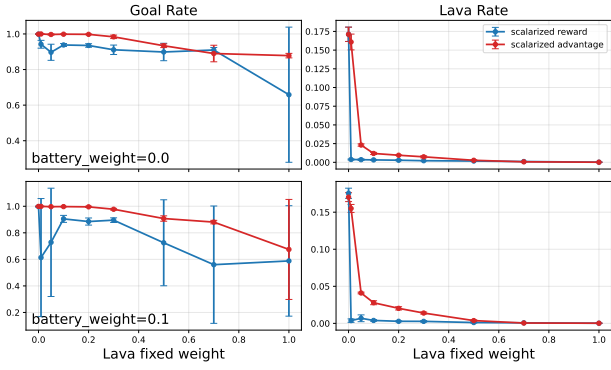


Figure 2. Final performance of GRPO policies evaluated over 1,000 episodes in the gridworld with fixed penalty weights, comparing *scalarized rewards* (blue) and *scalarized advantages* (red). Scalarized advantages consistently achieves higher goal-reaching rates while tracking the intended trade-off induced by the lava-weight sweep more faithfully, whereas scalarized rewards suppress lava visitation disproportionately.

bottom row in Fig. 2), *scalarized advantages* relaxes the lava rate for $\lambda_{\text{lava}}^{\text{fixed}} \leq 0.5$, whereas *scalarized rewards* behaves identically to the $\lambda_{\text{battery}}^{\text{fixed}} = 0.0$ setting, effectively optimizing the lava penalty in the same way regardless of the battery penalty.

Next, we compare the scalarization strategies in a constrained setting. In this experiment, we enforce constraint thresholds $\tilde{d}_{\text{lava}} = \tilde{d}_{\text{battery}} = 0.01$ and train for 512k episodes. In Appendix C.3, we show experiments with different threshold values. Figure 3 compares Constrained GRPO with *scalarized advantages* (ours) against a *scalarized rewards* baseline. Consistent with the fixed-weight results, scalarized advantages yields more stable learning across seeds (5 seeds), as reflected by the narrower shaded region throughout training (row 1). Moreover, scalarized advantages leads to richer behavior-rate dynamics (row 2, right column): the Lagrangian multipliers (row 3, right column) adapt to allow the constraint rates to increase toward the threshold, effectively encouraging the policy to use its available cost budget. On the other hand, scalarized rewards rapidly drives both constraint rates close to zero early in training (row 2, left column), and keeps them near-zero thereafter, even as the learned multipliers (row 3, left column) remain small.

This behavior can be understood through the implicit reweighting predicted by Theorem 4.1, and we refer to the effective scaling factors for the Z_j 's in Eqs. (5) and (6) as *effective weights*. Observe that despite the small learned multipliers λ_{lava} and λ_{battery} , the induced effective weights are larger and significantly noisier due to within-group variance and covariance effects (row 4, left column). This is especially problematic when the ordering of importance changes, as observed around 150K steps for the goal and lava weights

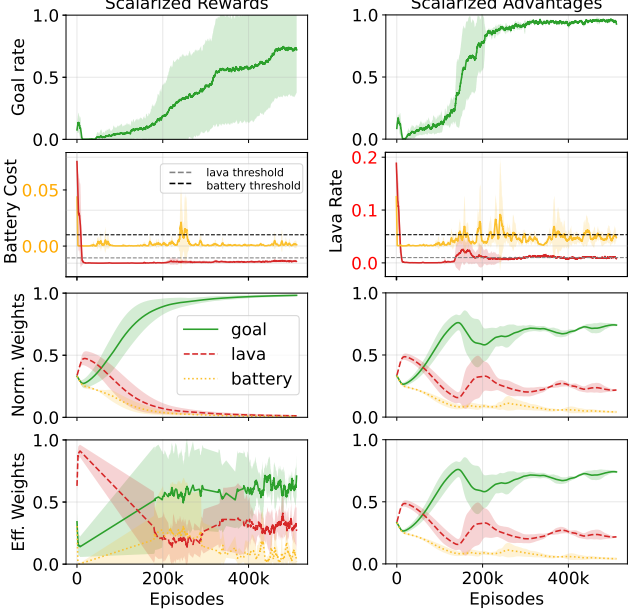


Figure 3. Learning dynamics on the gridworld under Constrained GRPO, comparing *scalarized rewards* (left) with *scalarized advantages* (right). Scalarized advantages yields more stable training and uses the available cost budget, with behavior rates adapting toward the specified thresholds as the Lagrangian multipliers adjust. In contrast, scalarized rewards collapses constraint rates toward near-zero early in training with the effective weights remaining larger and noisier despite small learned multipliers.

(red/green swap). Overall, these results support *scalarized advantages* as a more reliable advantage construction for Constrained GRPO, as it preserves the intended role of the Lagrangian multipliers in enforcing behavior specifications.

6. Robotics Environment

6.1. Benchmark Details

We focus our experiments on the NAVSIM-v2 driving benchmark (Cao et al., 2025), which contains 103k training scenarios (Navtrain) and 12k testing scenarios (Navtest) curated from OpenScene (Peng et al., 2023), a redistribution of the nuPlan dataset (Caesar et al., 2022). NAVSIM-v2 is well-suited for this study because it evaluates planning using explicit behavioural safety constraints alongside task-level objectives such as progress and comfort, enabling targeted analysis of behaviour specification. It focuses on the most challenging driving scenarios from the NAVSIM Challenge (Dauner et al., 2024), referred to as the *Navhard* split, and evaluates planners using a two-stage pseudo-simulation protocol. Stage 1 evaluates the policy's ability to drive in unseen nominal driving scenarios while stage 2 evaluates the policy's ability to produce corrective behaviors. More details can be found in Appendix D.

NAVSIM-v2 introduces the Extended PDM Score (EPDMS) as the primary metric to evaluate planners. EPDMS aggre-

Configuration Name	NC \uparrow	DAC \uparrow	DDC \uparrow	TLC \uparrow	Ego Progress \uparrow	Comfort \uparrow	EPDMS \uparrow	ADE@4s (m) \downarrow
PDM-Closed (privileged) (Dauner et al., 2023)	0.944	0.988	1.00	0.995	1.00	0.877	-	-
SFT Checkpoint	0.953	0.789	0.978	0.993	0.836	0.976	0.651	2.539
GRPO with EPDMS (Jaeger et al., 2025)	0.897	0.800	0.947	0.990	0.944	0.978	0.612	6.900
GRPO, ScRew, Equal Weights (Li et al., 2025b)	0.891	0.625	0.876	0.989	0.968	0.976	0.445	9.050
GRPO, ScAdv, Equal Weights (Ichihara et al., 2025)	0.908	0.661	0.900	0.989	0.954	0.973	0.490	7.172
GRPO, ScRew, Informed Weights	0.887	0.643	0.887	0.987	0.967	0.978	0.463	8.509
GRPO, ScAdv, Informed Weights	0.932	0.765	0.971	0.993	0.890	0.976	0.623	3.495
Constrained GRPO, ScRew	0.955	0.887	0.987	0.993	0.868	0.976	0.743	3.344
Constrained GRPO, ScAdv (ours)	0.957	0.928	0.989	0.998	0.796	0.977	0.774	3.361

Table 1. Stage 1 results on the NAVSIM-v2 Navhard split: We compare the different baseline reward function configurations and our proposed Constrained GRPO approach. *ScRew* stands for Scalarized rewards, while *ScAdv* stands for Scalarized Advantages. We can see that the best performing models are the constrained approaches, with our the *ScAdv* variant performing best on EPDMS.

gates multiple metrics via a product of hard penalty terms and a weighted average of auxiliary terms:

$$\text{EPDMS} = \underbrace{\prod_{m \in \mathcal{M}_{\text{pen}}} \text{filter}_m(\text{agent, human})}_{\text{penalty terms}} \cdot \underbrace{\left(\frac{\sum_{m \in \mathcal{M}_{\text{avg}}} w_m \text{filter}_m(\text{agent, human})}{\sum_{m \in \mathcal{M}_{\text{avg}}} w_m} \right)}_{\text{weighted average terms}}.$$

The penalty terms \mathcal{M}_{pen} include: (1) no at-fault collisions (NC), (2) drivable area compliance (DAC), (3) driving direction compliance (DDC), and (4) traffic light compliance (TLC). Since these penalties are combined multiplicatively, violating any one of them sets EPDMS to 0 for that scenario. To improve fairness, the function filter_m ignores penalty violations when the human expert driver also violates the same rule in the corresponding scene. The weighted average terms consist of: (1) ego progress along the route ($w_m = 5$), (2) time-to-collision ($w_m = 5$), (3) history comfort ($w_m = 2$), (4) extended comfort ($w_m = 2$), and (5) lane keeping ($w_m = 2$). The final EPDMS score lies in $[0, 1]$. In addition, we report the 4-second Average Displacement Error (ADE@4s) on Stage 1, computed with respect to the ground-truth trajectory. Although the penalty terms are designed as hard constraints at evaluation time, directly optimizing a multiplicative hard-gated objective can lead to sparse learning signals and unstable optimization, as we show. We therefore treat penalty terms as soft behavioural constraints, targeting near-perfect satisfaction (0.99) while preserving informative gradients throughout training.

6.2. Model Configurations

We initialize all experiments with the Qwen2.5-VL 3B Instruct model (Bai et al., 2025), which we pre-train following the Poutine supervised finetuning (SFT) recipe (Rowe et al., 2025). We then perform additional SFT on the NAVSIM training set (Cao et al., 2025; Dauner et al., 2024), reserving ≈ 11 k scenes as a held-out split for RL finetuning (RLFT). Further pre-training details appear in Appendix D.

For RLFT, we compare a set of GRPO-trained baselines.¹

(1) *GRPO with EPDMS*: we directly optimize EPDMS as the reward, analogous in spirit to CaRL (Jaeger et al., 2025) (which optimizes a similar objective with PPO). Because EPDMS is multiplicative, any violation of NC/DAC/DDC/TLC collapses the reward to zero, effectively acting as a hard constraint.

(2–5) *Linear scalarization*: we optimize a weighted sum of the three constraints and the weighted-average terms (WAT),

$$R(\tau) = w_1 \text{NC} + w_2 \text{DAC} + w_3 \text{DDC} + w_4 \text{WAT}.$$

This follows prior multi-objective GRPO setups (Ichihara et al., 2025; Li et al., 2025b). We evaluate both scalarization choices: scalarize rewards (*ScRew*) and scalarize advantages (*ScAdv*). We consider two weighting schemes: (i) equal weights $w_i = 0.25$ (*GRPO, ScRew/ScAdv, Equal Weights*), and (ii) an informed choice tuned from SFT behavior ($w_1=0.1$, $w_2=0.8$, $w_3=0.05$, $w_4=0.05$; *GRPO, ScRew/ScAdv, Informed Weights*).

(6–7) *Constrained GRPO*: we treat WAT as the main objective and enforce NC/DAC/DDC as constraints, setting all constraint satisfaction rate thresholds to 0.99². We again compare scalarized rewards and scalarized advantages (*Constrained GRPO, ScRew* vs. *Constrained GRPO, ScAdv*).

6.3. Results

Tables 1 and 2 report results on NAVSIM-v2 Stage 1 and Stage 2, respectively. For context, we also include the performance of the rule-based PDM planner (Dauner et al., 2023), whose trajectories are used to compute EPDMS. We now summarize the key findings.

Behavior specification through constrained RL outperforms alternative strategies. Overall, our results indicate

¹Traffic light compliance (TLC) was almost always satisfied in preliminary experiments and is therefore omitted as an explicit objective, except when optimizing EPDMS.

²Note that to maintain the upper-bound form of the constraint, we instead enforce a $\tilde{d}_k = 0.01$ threshold on the negation of the penalty terms NC/DAC/DDC.

Configuration Name	NC \uparrow	DAC \uparrow	DDC \uparrow	TLC \uparrow	Ego Progress \uparrow	Comfort \uparrow	EPDMS \uparrow
PDM-Closed (privileged) (Dauner et al., 2023)	0.881	0.906	0.963	0.985	1.00	0.915	-
SFT Checkpoint	0.800	0.756	0.869	0.981	0.878	0.963	0.444
GRPO with EPDMS (Jaeger et al., 2025)	0.749	0.759	0.829	0.969	0.979	0.945	0.381
GRPO, ScRew, Equal Weights (Li et al., 2025b)	0.751	0.696	0.787	0.968	0.986	0.954	0.347
GRPO, ScAdv, Equal Weights (Ichihara et al., 2025)	0.767	0.705	0.813	0.971	0.981	0.949	0.370
GRPO, ScRew, Informed Weights	0.754	0.695	0.791	0.969	0.986	0.954	0.350
GRPO, ScAdv, Informed Weights	0.778	0.731	0.831	0.972	0.944	0.962	0.385
Constrained GRPO, ScRew	0.810	0.784	0.866	0.976	0.939	0.952	0.436
Constrained GRPO, ScAdv (ours)	0.853	0.830	0.897	0.986	0.863	0.967	0.516

Table 2. **Stage 2 results on the NAVSIM-v2 Navhard split:** We compare the different baseline reward function configurations and our proposed Constrained GRPO approach. *ScRew* stands for Scalarized rewards, while *ScAdv* stands for Scalarized Advantages. We see significant improvement in the EPDMS score with our constrained GRPO with scalarized advantages approach.

that constrained RL provides a more effective mechanism for behavior specification than alternative reward-design approaches. In particular, the two constrained GRPO variants (bottom rows of Tables 1 and 2) achieve the strongest overall performance, with constrained GRPO using scalarized advantages attaining the highest EPDMS. On in-distribution Stage 1 driving scenarios, both constrained variants substantially improve upon the SFT checkpoint, whereas the unconstrained baselines do not consistently yield gains. On the more challenging out-of-distribution Stage 2 split, all methods exhibit degraded performance, as expected. Nevertheless, the constrained GRPO models remain the most competitive overall, showcasing the usefulness of our behavior specification framework for limiting bad driving behaviors.

Scalarized advantages outperforms scalarizing rewards. Across all three linear formulations (equal weights, informed weights, and constrained), scalarizing advantages yields consistently higher EPDMS than scalarizing rewards, for both Stage 1 and Stage 2. This trend aligns with our analysis in Section 4.2: when objective components have mismatched scales, scalarizing rewards can implicitly bias the optimization toward high-variance terms, distorting the intended trade-offs.

We further illustrate this effect in Figure 6 in Appendix D. Under constrained GRPO with scalarized rewards, the learned Lagrangian multipliers do not translate into effective constraint enforcement. This is most evident for drivable area compliance (DAC) and ego progress (EP), which is a proxy for the WAT objective: despite DAC being assigned nearly the maximum multiplier weight (and the main reward weight approaching zero), DAC does not reach the target satisfaction level, while EP continues to increase and only slowly decays later in training. In contrast, constrained GRPO with scalarized advantages responds rapidly to multiplier updates. DAC improves within the first ~ 1000 training steps, while EP decreases as its multiplier is reduced, demonstrating that the Lagrangian weights exert their intended influence on the learning dynamics. Finally, around ~ 2500 steps, the NC multiplier increases sharply as DAC

becomes satisfactory but collision compliance degrades, showing that the optimizer adaptively reallocates emphasis across constraints. Together, these dynamics corroborate our theoretical analysis, suggesting that scalarized advantages preserve the effectiveness of multiplier-based constraint enforcement.

Hard constraints lead to suboptimal learning dynamics. We also observe that directly optimizing EPDMS as a reward (i.e., GRPO with EPDMS) underperforms the soft-constraint formulations, yielding lower overall EPDMS on both Stage 1 and Stage 2. Intuitively, EPDMS couples constraints through a multiplicative structure, collapsing the learning signal whenever any penalty term is violated. This removes the ability to trade off and prioritize objectives smoothly during training, and prevents variance-aware balancing of component signals. In contrast, our soft-constraint formulation retains informative gradients even when constraints are partially violated, enabling more stable optimization and ultimately improved behavior specification.

7. Conclusion

We introduced Constrained GRPO, a Lagrangian extension of GRPO that enforces user-specified constraints via indicator costs and learned multipliers. We showed that naively *scalarizing rewards* before GRPO’s group normalization implicitly reweights objectives through within-group variance and covariance, undermining constraint enforcement. In contrast, *scalarizing advantages* preserves the intended role of the multipliers and yields a coherent learning signal for constrained optimization. Experiments in a controlled gridworld and on an autonomous driving benchmark confirm that Constrained GRPO with scalarized advantages trains more stably, achieves higher task performance, and satisfies constraints more faithfully. An interesting direction for future work is to couple Constrained GRPO with curriculum-style mechanisms that adapt constraint thresholds over training, potentially improving exploration and enabling satisfaction of stricter constraints.

8. Acknowledgements

We thank Samsung, the IVADO and the Canada First Research Excellence Fund (CFREF) / Apogee Funds, the Canada CIFAR AI Chairs Program, Fonds de Recherche Nature et Technologies (FRQNT), and the NSERC Discovery Grants program for their financial support. We thank Mila - Quebec AI Institute for compute resources. This research was supported by grants from NVIDIA and utilized NVIDIA 15K A100 GPU-hours on Saturn Cloud.

References

Achiam, J., Held, D., Tamar, A., and Abbeel, P. Constrained policy optimization. In *International Conference on Machine Learning*, pp. 22–31. PMLR, 2017.

Altman, E. *Constrained Markov decision processes*, volume 7. CRC Press, 1999.

Arai, H., Miwa, K., Sasaki, K., Yamaguchi, Y., Watanabe, K., Aoki, S., and Yamamoto, I. Covla: Comprehensive vision-language-action dataset for autonomous driving. *2025 IEEE/CVF Winter Conference on Applications of Computer Vision (WACV)*, pp. 1933–1943, 2024. URL <https://api.semanticscholar.org/CorpusID:271909725>.

Bai, S., Chen, K., Liu, X., Wang, J., Ge, W., Song, S., Dang, K., Wang, P., Wang, S., Tang, J., Zhong, H., Zhu, Y., Yang, M., Li, Z., Wan, J., Wang, P., Ding, W., Fu, Z., Xu, Y., Ye, J., Zhang, X., Xie, T., Cheng, Z., Zhang, H., Yang, Z., Xu, H., and Lin, J. Qwen2.5-vl technical report. *ArXiv*, abs/2502.13923, 2025. URL <https://api.semanticscholar.org/CorpusID:276449796>.

Bai, Y., Kadavath, S., Kundu, S., Askell, A., Kernion, J., Jones, A., Chen, A., Goldie, A., Mirhoseini, A., McKinnon, C., Chen, C., Olsson, C., Olah, C., Hernandez, D., Drain, D., Ganguli, D., Li, D., Tran-Johnson, E., Perez, E., Kerr, J., Mueller, J., Ladish, J., Landau, J., Ndousse, K., Lukosuite, K., Lovitt, L., Sellitto, M., Elhage, N., Schiefer, N., Mercado, N., Dassarma, N., Lasenby, R., Larson, R., Ringer, S., Johnston, S., Kravec, S., Showk, S. E., Fort, S., Lanham, T., Telleen-Lawton, T., Conerly, T., Henighan, T. J., Hume, T., Bowman, S., Hatfield-Dodds, Z., Mann, B., Amodei, D., Joseph, N., McCandlish, S., Brown, T. B., and Kaplan, J. Constitutional ai: Harmlessness from ai feedback. *ArXiv*, abs/2212.08073, 2022. URL <https://api.semanticscholar.org/CorpusID:254823489>.

Caesar, H., Kabzan, J., Tan, K. S., Fong, W. K., Wolff, E., Lang, A., Fletcher, L., Beijbom, O., and Omari, S. Nuplan: A closed-loop ml-based planning benchmark for autonomous vehicles, 2022. URL <https://arxiv.org/abs/2106.11810>.

Cao, W., Hallgarten, M., Li, T., Dauner, D., Gu, X., Wang, C., Miron, Y., Aiello, M., Li, H., Gilitschenski, I., Ivanovic, B., Pavone, M., Geiger, A., and Chitta, K. Pseudo-simulation for autonomous driving. In *Conference on Robot Learning (CoRL)*, 2025.

Chen, K., Sun, W., Cheng, H., and Zheng, S. Rift: Group-relative rl fine-tuning for realistic and controllable traffic simulation, 2025. URL <https://arxiv.org/abs/2505.03344>.

Christiano, P., Leike, J., Brown, T. B., Martic, M., Legg, S., and Amodei, D. Deep reinforcement learning from human preferences. *arXiv preprint arXiv:1706.03741*, 2017.

Chu, T., Zhai, Y., Yang, J., Tong, S., Xie, S., Schuurmans, D., Le, Q. V., Levine, S., and Ma, Y. Sft memorizes, rl generalizes: A comparative study of foundation model post-training. *ArXiv*, abs/2501.17161, 2025. URL <https://api.semanticscholar.org/CorpusID:275932560>.

Cobbe, K., Kosaraju, V., Bavarian, M., Chen, M., Jun, H., Kaiser, L., Plappert, M., Tworek, J., Hilton, J., Nakano, R., et al. Training verifiers to solve math word problems. *arXiv preprint arXiv:2110.14168*, 2021.

Dai, J., Pan, X., Sun, R., Ji, J., Xu, X., Liu, M., Wang, Y., and Yang, Y. Safe rlhf: Safe reinforcement learning from human feedback. *ArXiv*, abs/2310.12773, 2023. URL <https://api.semanticscholar.org/CorpusID:264306078>.

Dauner, D., Hallgarten, M., Geiger, A., and Chitta, K. Parting with misconceptions about learning-based vehicle motion planning. In *Conference on Robot Learning*, pp. 1268–1281. PMLR, 2023.

Dauner, D., Hallgarten, M., Li, T., Weng, X., Huang, Z., Yang, Z., Li, H., Gilitschenski, I., Ivanovic, B., Pavone, M., Geiger, A., and Chitta, K. Navsim: Data-driven non-reactive autonomous vehicle simulation and benchmarking. In *Advances in Neural Information Processing Systems (NeurIPS)*, 2024.

Goodfellow, I., Pouget-Abadie, J., Mirza, M., Xu, B., Warde-Farley, D., Ozair, S., Courville, A., and Bengio, Y. Generative adversarial nets. *Advances in neural information processing systems*, 27, 2014.

Goyal, P., Niekum, S., and Mooney, R. J. Using natural language for reward shaping in reinforcement learning. *arXiv preprint arXiv:1903.02020*, 2019.

Haarnoja, T., Zhou, A., Hartikainen, K., Tucker, G., Ha, S., Tan, J., Kumar, V., Zhu, H., Gupta, A., Abbeel, P., et al. Soft actor-critic algorithms and applications. *arXiv preprint arXiv:1812.05905*, 2018.

Hadfield-Menell, D., Milli, S., Abbeel, P., Russell, S., and Dragan, A. Inverse reward design. *arXiv preprint arXiv:1711.02827*, 2017.

Ichihara, Y., Jinnai, Y., Morimura, T., Sakamoto, M., Mitsuhashi, R., and Uchibe, E. Mo-grpo: Mitigating reward hacking of group relative policy optimization on multi-objective problems. *arXiv preprint arXiv:2509.22047*, 2025.

Jaeger, B., Dauner, D., Beißwenger, J., Gerstenecker, S., Chitta, K., and Geiger, A. Carl: Learning scalable planning policies with simple rewards. *arXiv preprint arXiv:2504.17838*, 2025.

Ji, J., Chen, X., Pan, R., Zhu, H., Zhang, C., Li, J., Hong, D., Chen, B., Zhou, J., Wang, K., Dai, J., Chan, C.-M., Han, S., Guo, Y., and Yang, Y. Safe rlhf-v: Safe reinforcement learning from human feedback in multi-modal large language models. *ArXiv*, abs/2503.17682, 2025. URL <https://api.semanticscholar.org/CorpusID:277271998>.

Korpelevich, G. An extragradient method for finding saddle points and for other problems. 1976.

Lewkowycz, A., Andreassen, A., Dohan, D., Dyer, E., Michalewski, H., Ramasesh, V. V., Slone, A., Anil, C., Schlag, I., Gutman-Solo, T., Wu, Y., Neyshabur, B., Gur-Ari, G., and Misra, V. Solving quantitative reasoning problems with language models. *ArXiv*, abs/2206.14858, 2022. URL <https://api.semanticscholar.org/CorpusID:250144408>.

Li, T., Qiu, Y., Wu, Z., Lindström, C., Su, P., Nießner, M., and Li, H. Mtgs: Multi-traversal gaussian splatting. *arXiv preprint arXiv:2503.12552*, 2025a.

Li, X., Li, Z., Kosuga, Y., and Bian, V. Optimizing safe and aligned language generation: A multi-objective grpo approach. *ArXiv*, abs/2503.21819, 2025b. URL <https://api.semanticscholar.org/CorpusID:277435738>.

Li, Y., Tian, M., Zhu, D., Zhu, J., Lin, Z., Xiong, Z., and Zhao, X. Drive-r1: Bridging reasoning and planning in vlms for autonomous driving with reinforcement learning. *ArXiv*, abs/2506.18234, 2025c. URL <https://api.semanticscholar.org/CorpusID:279999326>.

Lin, T., Jin, C., and Jordan, M. On gradient descent ascent for nonconvex-concave minimax problems. In *International Conference on Machine Learning*, pp. 6083–6093. PMLR, 2020.

Liu, S.-Y., Dong, X., Lu, X., Diao, S., Belcak, P., Liu, M., Chen, M.-H., Yin, H., Wang, Y.-C. F., Cheng, K.-T., et al. Gdpo: Group reward-decoupled normalization policy optimization for multi-reward rl optimization. *arXiv preprint arXiv:2601.05242*, 2026.

MacGlashan, J., Babes-Vroman, M., desJardins, M., Littman, M. L., Muresan, S., Squire, S., Tellex, S., Arumugam, D., and Yang, L. Grounding english commands to reward functions. In *Robotics: Science and Systems*, 2015.

Mindermann, S., Shah, R., Gleave, A., and Hadfield-Menell, D. Active inverse reward design. *arXiv preprint arXiv:1809.03060*, 2018.

Moskovitz, T., Singh, A. K., Strouse, D., Sandholm, T., Salakhutdinov, R., Dragan, A. D., and McAleer, S. M. Confronting reward model overoptimization with constrained rlhf. *ArXiv*, abs/2310.04373, 2023. URL <https://api.semanticscholar.org/CorpusID:263829192>.

Ouyang, L., Wu, J., Jiang, X., Almeida, D., Wainwright, C. L., Mishkin, P., Zhang, C., Agarwal, S., Slama, K., Ray, A., Schulman, J., Hilton, J., Kelton, F., Miller, L., Simens, M., Askell, A., Welinder, P., Christiano, P., Leike, J., and Lowe, R. Training language models to follow instructions with human feedback, 2022. URL <https://arxiv.org/abs/2203.02155>.

Pei, M., Shi, S., and Shen, S. Advancing multi-agent traffic simulation via r1-style reinforcement fine-tuning. *ArXiv*, abs/2509.23993, 2025. URL <https://api.semanticscholar.org/CorpusID:281675127>.

Peng, S., Genova, K., Jiang, C. M., Tagliasacchi, A., Pollefeys, M., and Funkhouser, T. Openscene: 3d scene understanding with open vocabularies, 2023. URL <https://arxiv.org/abs/2211.15654>.

Polyak, B. Iterative methods using lagrange multipliers for solving extremal problems with constraints of the equation type. *USSR Computational Mathematics and Mathematical Physics*, 10(5):42–52, 1970.

Ratner, E., Hadfield-Menell, D., and Dragan, A. D. Simplifying reward design through divide-and-conquer. *arXiv preprint arXiv:1806.02501*, 2018.

Ray, A., Achiam, J., and Amodei, D. Benchmarking safe exploration in deep reinforcement learning. *arXiv preprint arXiv:1910.01708*, 7, 2019.

Rowe, L., de Schaezen, R., Girgis, R., Pal, C., and Paull, L. Poutine: Vision-language-trajectory pre-training and reinforcement learning post-training enable robust end-to-end autonomous driving, 2025. URL <https://arxiv.org/abs/2506.11234>.

Roy, J., Girgis, R., Romoff, J., Bacon, P.-L., and Pal, C. J. Direct behavior specification via constrained reinforcement learning. In *International Conference on Machine Learning*, 2021. URL <https://api.semanticscholar.org/CorpusID:245424738>.

Saunders, W., Sastry, G., Stuhlmüller, A., and Evans, O. Trial without error: Towards safe reinforcement learning via human intervention. *arXiv preprint arXiv:1707.05173*, 2017.

Schulman, J., Wolski, F., Dhariwal, P., Radford, A., and Klimov, O. Proximal policy optimization algorithms. *arXiv preprint arXiv:1707.06347*, 2017.

Shao, Z., Wang, P., Zhu, Q., Xu, R., Song, J.-M., Zhang, M., Li, Y. K., Wu, Y., and Guo, D. Deepseekmath: Pushing the limits of mathematical reasoning in open language models. *ArXiv*, abs/2402.03300, 2024. URL <https://api.semanticscholar.org/CorpusID:267412607>.

Stooke, A., Achiam, J., and Abbeel, P. Responsive safety in reinforcement learning by pid lagrangian methods. In *International Conference on Machine Learning*, pp. 9133–9143. PMLR, 2020.

Sutton, R. S. and Barto, A. G. *Reinforcement learning: An introduction*. MIT press, 2018.

Treiber, M., Hennecke, A., and Helbing, D. Congested traffic states in empirical observations and microscopic simulations. *Physical review E*, 62(2):1805, 2000.

Uzawa, H., Anow, K., and Hurwicz, L. Studies in linear and nonlinear programming, 1958.

Wang, H., Xiong, W., Xie, T., Zhao, H., and Zhang, T. Interpretable preferences via multi-objective reward modeling and mixture-of-experts. In *Conference on Empirical Methods in Natural Language Processing*, 2024. URL <https://api.semanticscholar.org/CorpusID:270562658>.

Wang, Y., Luo, W., Bai, J., Cao, Y., Che, T., Chen, K., Chen, Y., Diamond, J., Ding, Y., Ding, W., et al. Alpamayo-r1: Bridging reasoning and action prediction for generalizable autonomous driving in the long tail. *arXiv preprint arXiv:2511.00088*, 2025.

Wei, J., Wang, X., Schuurmans, D., Bosma, M., Chi, E. H., Xia, F., Le, Q., and Zhou, D. Chain of thought prompting elicits reasoning in large language models. *ArXiv*, abs/2201.11903, 2022. URL <https://api.semanticscholar.org/CorpusID:246411621>.

Zhang, B., Zhang, Y., Ji, J., Lei, Y., Dai, J., Chen, Y., and Yang, Y. Safevla: Towards safety alignment of vision-language-action model via safe reinforcement learning. *ArXiv*, abs/2503.03480, 2025a. URL <https://api.semanticscholar.org/CorpusID:276782535>.

Zhang, B., Zhang, Y., Ji, J., Lei, Y., Dai, J., Chen, Y., and Yang, Y. Safevla: Towards safety alignment of vision-language-action model via constrained learning. *arXiv preprint arXiv:2503.03480*, 2025b.

Zhang, Y., Vuong, Q., and Ross, K. W. First order constrained optimization in policy space. *arXiv preprint arXiv:2002.06506*, 2020.

Zheng, B., Verma, S., Zhou, J., Tsang, I., and Chen, F. Imitation learning: Progress, taxonomies and opportunities. *arXiv preprint arXiv:2106.12177*, 2021.

A. Proof of Theorem 4.1

Theorem A.1 (Theorem 4.1 (restated)). *Let*

$$\mathbf{x} := \begin{bmatrix} R \\ C_1 \\ \vdots \\ C_K \end{bmatrix} \in \mathbb{R}^{K+1}, \quad \boldsymbol{\lambda} := \begin{bmatrix} \lambda_R \\ \lambda_1 \\ \vdots \\ \lambda_K \end{bmatrix} \in \mathbb{R}^{K+1},$$

and define the scalarized reward $R_S := \boldsymbol{\lambda}^\top \mathbf{x}$. Denote the within-group mean and covariance of \mathbf{x} by $\boldsymbol{\mu} := \mathbb{E}[\mathbf{x}]$ and $\boldsymbol{\Sigma} := \text{Cov}(\mathbf{x})$, and let $\sigma_{R_S} := \sqrt{\text{Var}(R_S)} = \sqrt{\boldsymbol{\lambda}^\top \boldsymbol{\Sigma} \boldsymbol{\lambda}}$. Further define per-component standardizations

$$\mathbf{Z} := \mathbf{D}^{-1}(\mathbf{x} - \boldsymbol{\mu}), \quad \mathbf{D} := \text{diag}(\sigma_R, \sigma_{C_1}, \dots, \sigma_{C_K})$$

$$\sigma_R > 0, \quad \sigma_{C_k} > 0 \quad \forall k \in \{1, \dots, K\}$$

so that

$$Z_R := \frac{R - \mu_R}{\sigma_R},$$

$$Z_{C_k} := \frac{C_k - \mu_{C_k}}{\sigma_{C_k}}, \quad k = 1, \dots, K, \quad (7)$$

where $\mu_{(\cdot)}$ and $\sigma_{(\cdot)}$ denote the within-group mean and standard deviation of the corresponding component. Then the GRPO advantage obtained by standardizing the scalarized reward,

$$A_{\text{ScRew}} := \frac{R_S - \mathbb{E}[R_S]}{\sigma_{R_S}},$$

admits the expansion

$$A_{\text{ScRew}} = \frac{(\mathbf{D}\boldsymbol{\lambda})^\top \mathbf{Z}}{\sigma_{R_S}} = \sum_{j=0}^K \left(\frac{\lambda_j \sigma_j}{\sigma_{R_S}} \right) Z_j, \quad (8)$$

where we index $j = 0$ as the main reward component ($\lambda_0 \equiv \lambda_R$, $\sigma_0 \equiv \sigma_R$) and $j = k$ corresponds to cost C_k . Consequently, the effective contribution of each standardized component Z_j is scaled by $\lambda_j \sigma_j / \sigma_{R_S}$, and therefore depends on within-group scales and (through σ_{R_S}) the full covariance structure $\boldsymbol{\Sigma}$.

Proof. By definition, $R_S = \boldsymbol{\lambda}^\top \mathbf{x}$ and $\mathbb{E}[R_S] = \boldsymbol{\lambda}^\top \boldsymbol{\mu}$, hence

$$R_S - \mathbb{E}[R_S] = \boldsymbol{\lambda}^\top (\mathbf{x} - \boldsymbol{\mu}). \quad (9)$$

Moreover,

$$\text{Var}(R_S) = \text{Var}(\boldsymbol{\lambda}^\top \mathbf{x}) = \boldsymbol{\lambda}^\top \text{Cov}(\mathbf{x}) \boldsymbol{\lambda} = \boldsymbol{\lambda}^\top \boldsymbol{\Sigma} \boldsymbol{\lambda},$$

which yields $\sigma_{R_S} = \sqrt{\boldsymbol{\lambda}^\top \boldsymbol{\Sigma} \boldsymbol{\lambda}}$.

Next, from the definition of \mathbf{Z} , we have $\mathbf{x} - \boldsymbol{\mu} = \mathbf{D}\mathbf{Z}$. Substituting into Eq. (9) gives

$$R_S - \mathbb{E}[R_S] = \boldsymbol{\lambda}^\top \mathbf{D}\mathbf{Z} = (\mathbf{D}\boldsymbol{\lambda})^\top \mathbf{Z}.$$

Dividing both sides by σ_{R_S} yields

$$A_{\text{ScRew}} = \frac{R_S - \mathbb{E}[R_S]}{\sigma_{R_S}} = \frac{(\mathbf{D}\boldsymbol{\lambda})^\top \mathbf{Z}}{\sigma_{R_S}},$$

which is the first equality in Eq. (8). Expanding the dot product gives the summation form

$$A_{\text{ScRew}} = \sum_{j=0}^K \left(\frac{\lambda_j \sigma_j}{\sigma_{R_S}} \right) Z_j,$$

completing the proof. \square

B. Numerical Example of Theorem 4.1

We provide a simple 1-constraint example to understand the difference in practice. Let $\lambda_R = 0.3$ and $\lambda_C = 0.7$ (since both must sum to 1), $\sigma_R = 0.5$, $\sigma_C = 0.2$, and $\rho = 0.1$. Then we can compute the standard deviation of the combined signal with scalarized rewards as

$$\begin{aligned}\sigma_{RS} &= \sqrt{(0.3^2 \cdot 0.5^2) + (0.7^2 \cdot 0.2^2) + (2 \cdot 0.3 \cdot 0.7 \cdot 0.1 \cdot 0.5 \cdot 0.2)} \\ &\approx 0.215174.\end{aligned}$$

With σ_{RS} , the effective weights on (Z_R, Z_C) :

$$\begin{aligned}\text{Scalarized Advantages: } &(0.3, 0.7), \\ \text{Scalarized Rewards: } &\left(\frac{0.3 \cdot 0.5}{0.215174}, \frac{0.7 \cdot 0.2}{0.215174}\right) \approx (0.697, 0.651).\end{aligned}$$

As we can see from this simple example, the reward term was 2.33 times less important according to the current Lagrangian multipliers. However, the 2nd approach effectively scales its coefficient to be even more important than the constraint.

With this, we conclude that if you want λ to faithfully encode your intended reward–constraint trade-off independently of group scales and covariance, the per-component standardization followed by combining terms using λ is the more faithful approach. In general, the second approach is not invalid but has the caveat that it implicitly reweights the multipliers by the components’ standard deviations (and ρ). This results in agents effectively having to satisfy the high-variance components first prior to satisfying the low-variance ones, *regardless of the Lagrangian multiplier λ_i values*. In our experiments in Section 6, we present results on a toy environment and in the real-world Navsim driving benchmark, comparing both approaches with fixed and varying Lagrangian multipliers.

C. Gridworld Environment

C.1. Environment Details

Our gridworld is a 10×10 grid in which the agent is initialized uniformly at random and must navigate to a randomly sampled goal location. Reaching the goal yields a sparse terminal reward of 1.0. At the start of each episode, 20% of the tiles are designated as lava; stepping onto a lava tile incurs a penalty of 1.0 (i.e., a cost). The agent is also equipped with a battery that drains by 5% at every timestep and incurs a penalty whenever its charge falls below 10%. The action space consists of five discrete actions: moving in the four cardinal directions, or staying in place to recharge at a rate of 20% per timestep. The agent observes a compact state representation consisting of:

- its (x, y) position, normalized to $[0, 1]^2$;
- the goal (x, y) coordinates, normalized to $[0, 1]^2$;
- the current battery level in $[0, 1]$;
- a 5×5 local occupancy map centered on the agent, where entries indicate lava tiles (flattened to a 25-dimensional vector).

Episodes last at most 80 timesteps and terminate early only upon reaching the goal.

C.2. Implementation Details

We train a categorical policy parameterized by a two-layer MLP (hidden size 128 with ReLU activations) that outputs action logits. Policies are optimized with the GRPO clipped objective ($\epsilon = 0.2$) using 2 epochs per update, minibatches of size 2048, and an entropy bonus of 0.001. Training runs for 8000 update steps; each update collects 64 episodes via grouped rollouts (group size 8 across 8 groups). We use Adam for the policy optimizer (learning rate 5×10^{-4} by default) and, when constraints are enabled, a separate Adam optimizer for cost weights (learning rate 10^{-2}). Cost weights are parameterized via a softmax over $\{\text{reward}, \text{lava}, \text{battery}\}$ parameters and updated every step and initialized to 0.02 logits.

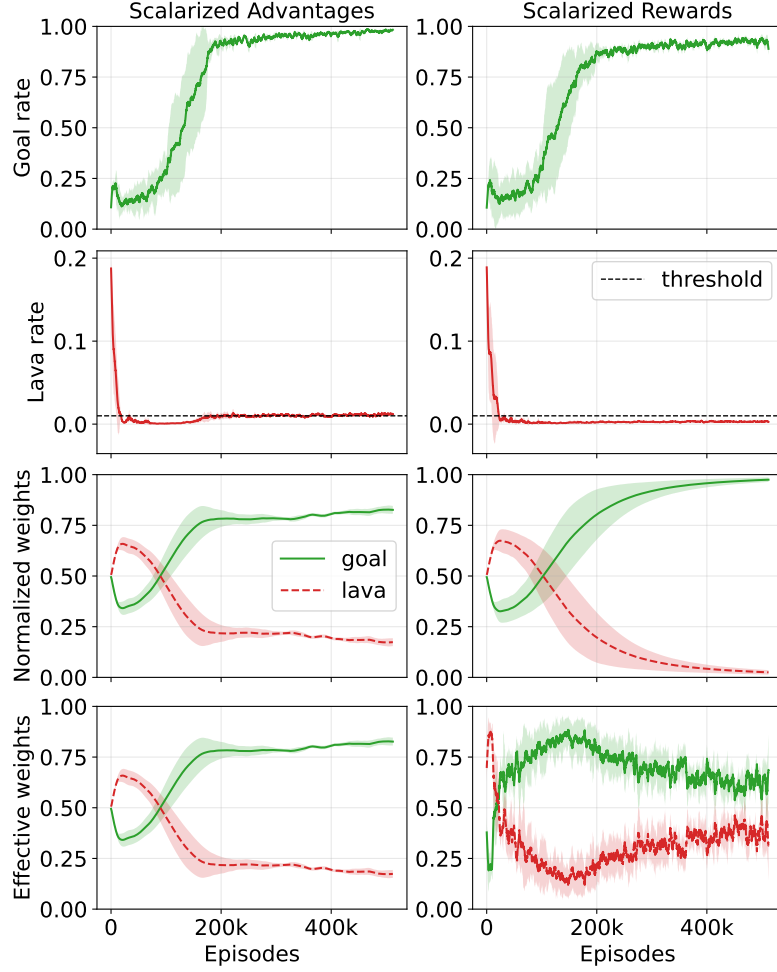


Figure 4. Learning dynamics on the gridworld under Constrained GRPO, comparing *scalarized advantages* (left) and *scalarized rewards* (right). In this experiment, we set $\tilde{d}_{\text{lava}} = 0.01$ and do not enforce the battery constraint. Scalarized advantages again produces a stronger final policy and makes effective use of the allowable cost budget, with the lava rate touching the specified threshold in order to allow for success on the main task. In contrast, scalarized rewards drives the constraint rate to near-zero early in training; despite small multipliers values, the corresponding effective weights remain larger and noisier, leading to less stable learning and lower final performance.

C.3. Additional Constrained Optimization Experiments

We include additional results comparing scalarizing rewards with scalarizing advantages for a single constraint in Figure 4, and with both battery and lava constraints in Figure 5. We refer the reader to the caption for more details.

D. NAVSIM v2

D.1. Dataset Details

In Stage 1, the benchmark evaluates closed-loop planning quality in an open-loop manner. Concretely, each planner outputs a 4-second trajectory sampled at 10 Hz, which is then executed forward without feedback using a kinematic bicycle model with an LQR controller. Unlike NAVSIM-v1 (Dauner et al., 2024), which simply replayed recorded agent trajectories, NAVSIM-v2 introduces reactive behavior from other vehicles through the Intelligent Driver Model (IDM) (Treiber et al., 2000), improving simulation realism. Stage 2 evaluates robustness under compounding error by synthesizing new driving rollouts using Multi-Traversal Gaussian Splatting (Li et al., 2025a). These scenarios are initialized from perturbed ego states (e.g., suboptimal position and/or heading), requiring the planner to produce corrective behavior. The resulting Navhard evaluation split contains 450 observations for Stage 1 and 5,462 observations for Stage 2.

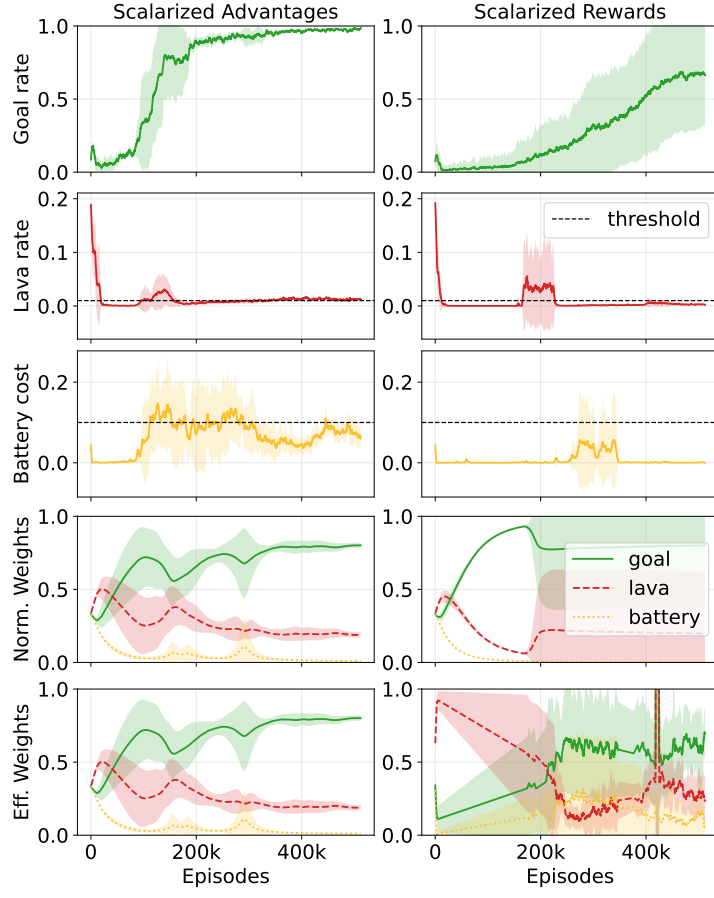


Figure 5. Learning dynamics on the gridworld under Constrained GRPO, comparing *scalarized advantages* (left) and *scalarized rewards* (right). In this experiment, we set $\tilde{d}_{\text{lava}} = 0.01$ and $\tilde{d}_{\text{battery}} = 0.1$. Scalarized advantages again produces a stronger final policy and makes effective use of its allowable costs’ budget, with both the lava rate and battery rate stabilizing near their specified thresholds in order to allow for success on the main task. In contrast, scalarizing rewards drives both constraints’ cost rate to near-zero early in training. Even with small values of multipliers, the corresponding effective weights remain larger and noisier, leading to less stable learning and lower final performance. Interestingly, we see that when it tries to creep higher, the effective multipliers react excessively, resulting in the agent not adequately navigating the environment, as shown by the poor goal success rate.

D.2. Base Model Pretraining

We initialize all experiments from the Qwen2.5-VL 3B Instruct vision-language model (Bai et al., 2025). We first perform supervised finetuning on the CoVLA dataset (Arai et al., 2024), which contains 83 hours of nominal driving collected in Japan. Following Rowe et al. (Rowe et al., 2025), we represent planned trajectories as serialized text and train the model using next-token prediction in the original vocabulary.

To promote richer planning behavior, we additionally include automatically generated chain-of-thought annotations, produced in a zero-shot manner by Qwen2.5-VL 72B Instruct, and prepend these to the target trajectory sequences during training. After this initialization stage, we further supervise finetune the model on 92,000 scenes from the NAVSIM training set (Cao et al., 2025; Dauner et al., 2024). The remaining $\approx 11,000$ scenes are held out and used exclusively for reinforcement learning finetuning (RLFT) in our benchmark experiments.

D.3. Hyperparameters

We finetune all our models for two epochs through the 11k held-out scenes for RL finetuning (RLFT). All our experiments are performed on 8 A100 GPUs, with each RLFT run taking nearly 20 hours. We set $\beta = 0.02$ to constrain the policy to the reference SFT policy, the learning rate to $1e^{-6}$, and the group size to 16. We perform two iterations of policy optimization per batch of data. We update the Lagrangian multipliers at the same rate as the policy.

D.4. Additional Results

In Figure 6, we show representative learning dynamics of the multipliers and corresponding constraints, highlighting differences between the two advantage estimation approaches for constrained GRPO in NAVSIM.

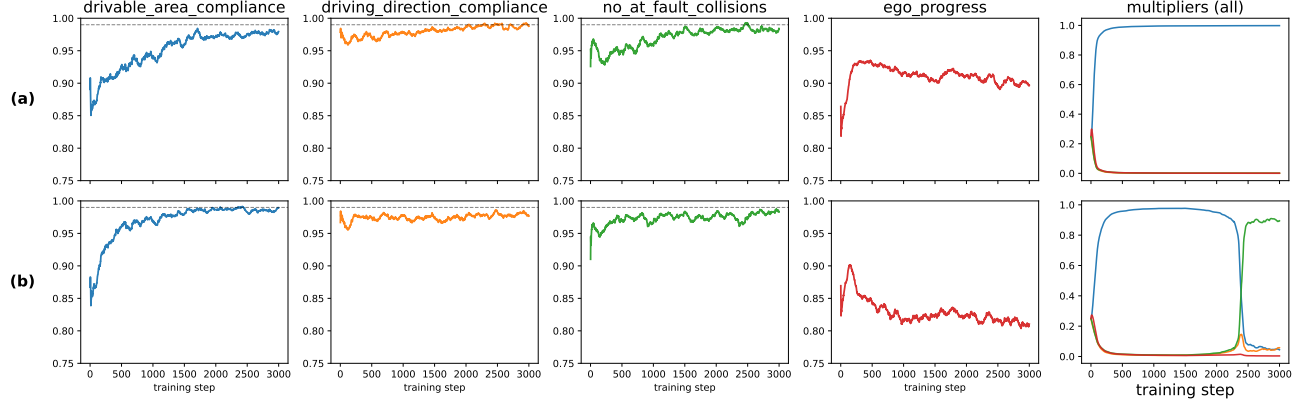


Figure 6. Constrained GRPO plots of constraint and multiplier values through training, comparing (a) scalarized rewards with (b) scalarized advantages. Focusing on the ego progress and the drivable area compliance, we see that with the scalarized rewards, the policy does not adhere to the multiplier settings as we intend. First, the drivable area compliance (DAC) stays below its minimum threshold 0.99 throughout its training even though the multiplier value had moved close to its maximum value of 1.0. Moreover, we see that even though the ego-progress (a component of the WAT reward) is set to a very low value, the scalarized rewards variant still maximizes it. Conversely, the scalarized advantage model allows the different components to adhere to the multiplier setting. In addition, we see that at around 2500 training steps, something interesting happens in the scalarized advantage model's multipliers; since the DAC constraint is satisfied and the no at-fault collision (NC) takes a sharp dip, the Lagrangian optimization pushes the NC multiplier higher and squashes the DAC multiplier. This confirms our theoretical findings that scalarizing the advantages leads to better adherence to the specified multiplier weights.